Results from Laser Sheet Visualization of a Periodic Rotor Wake

A. Brand,* N. Komerath,† and H. McMahon‡
Georgia Institute of Technology, Atlanta, Georgia

A laser sheet has been applied to the visualization of a periodic rotor wake produced by a model rotorcraft in forward flight. A stiff, two-bladed teetering rotor is mounted independently of an idealized airframe consisting of an instrumented circular cylinder with a hemispherical nose. The model was installed in a wind tunnel, and tests were carried out at three different advance ratios (forward flight speeds) at one value of rotor collective pitch angle. The laser sheet technique enables detailed flow visualization to be carried out. Quantitative data regarding the location of the rotor tip vortex can be obtained. Results from the flow visualization confirm that the rotor wake is a complex flowfield not amenable to simple analysis. However, the details of the tip vortex geometry are both periodic and repeatable. The motion of the rotor wake in close proximity to the airframe is examined. The behavior of the tip vortex is strongly affected by the presence of the airframe. In particular, the interaction of the rotor tip vortex with the airframe results in the destruction of the vortex core; apparently the vorticity is diffused, and the vortex loses its definition. No vortex filaments appear below the airframe as identifiable flow features. Examples of airframe surface pressure data are presented and are seen to correlate well with the results from the flow visualization.

Nomenclature

b	= number of blades (2)
C_p	= pressure coefficient, $(P - P_\infty)/q_\infty$
C_T	= thrust coefficient, $T/\rho\pi\Omega^2R^4$
c	= blade chord
P	= mean static pressure
P_∞	= test section freestream static pressure
q_∞	= freestream dynamic pressure, $\rho V_\infty^2/2$
R,T	= rotor radius and thrust, respectively
V_∞	= tunnel freestream velocity
X,Y,Z	= streamwise, transverse, and vertical coordinates, respectively.
μ	= advance ratio, $V_\infty/\Omega R$
ρ	= density of air
σ	= rotor solidity, blade area/πR^2
Ψ	= rotor blade azimuth angle, deg
Ω	= rotor shaft angular velocity, rad/s

Introduction

THE vortical wake of a helicopter rotor in forward flight creates an extremely complex flowfield that is difficult to model analytically or to study experimentally. The wake flow is unsteady and asymmetric and can contain large amounts of energy in the tip vortices that are shed from the rotor blades. The airframe and the rotor have a mutual aerodynamic interference one with the other which, in turn, is reflected in the behavior of the wake. The helicopter in forward flight thus represents a challenging problem in aerodynamics, which must be better understood if significant advances are to be made in such areas as helicopter performance and handling qualities.[1,2]

As a research task in the Rotary Wing Center at Georgia Institute of Technology, an experimental study was undertaken, aimed at gaining physical insights regarding the role of the rotor wake in forward flight. These experimental investigations furnish a comprehensive data base that will be useful in the formulation and evaluation of prediction codes now being developed.[3]

The experimental testing involves the use of an idealized model rotor and airframe mounted in the John J. Harper 2.31 × 2.74-m wind tunnel at Georgia Institute of Technology. Extensive measurements of both mean and periodic surface pressure distributions on the airframe have been made, and the boundaries of the rotor wake have been determined.[4,5] A laser velocimeter has been used to make detailed flow velocity measurements near the rotor tip path plane and in the wake flow between the rotor and the airframe.[6] These measurements are very time consuming, and a method was sought that would allow visualization of the rotor wake to guide the placement of the data-taking grids at points away from the surface of the airframe. This also would enhance the interpretation of surface pressure measurements.

Laser sheet visualization of steady flowfields has been used successfully for several years.[7-9] By building on this background, a laser sheet technique was developed for visualizing the periodic wake flow between the model rotor and the airframe. More precisely, the vortices emanating from the tips of the rotor blades were made visible. This technique involves the strobing of the laser sheet, with data collected by means of a video camera and reduced in a quantitative fashion by using a monitor and a superimposed spatial grid. The details of this visualization method are found in Ref. 10.

During the development of the laser sheet visualization technique for this study, it became apparent that knowledge of the location and behavior of the blade tip vortices provided many insights into the physical features of the flow, allowing improved physical interpretation of the surface pressure data. The visualization results reported here are intended to show the kinds of data that can be obtained from the laser sheet method. Furthermore, correlations with other measurements are presented to illustrate how knowledge from flow visualization can enhance the interpretation of other data and lead to a better understanding of the aerodynamics of the helicopter in forward flight.

Presented as Paper 88-0192 at the AIAA 26th Aerospace Sciences Meeting, Reno, NV, Jan. 11-14, 1988; received Feb. 7, 1988.

*Graduate Research Fellow, School of Aerospace Engineering. Member AIAA.

†Assistant Professor, School of Aerospace Engineering. Member AIAA.

‡Professor, School of Aerospace Engineering. Senior Member AIAA.

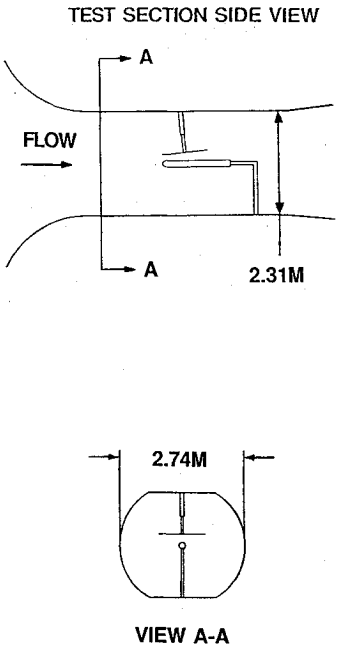

Fig. 1 Rotor-airframe installation schematic.

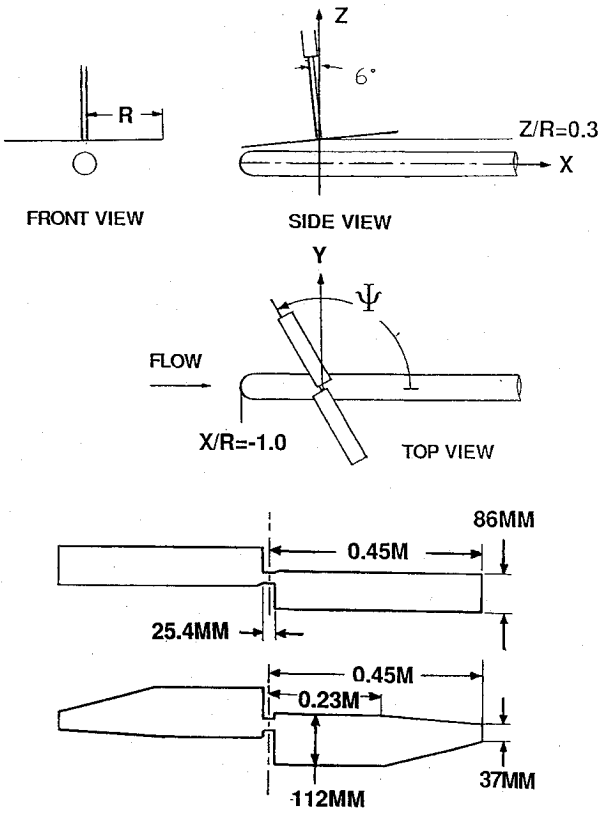

Fig. 2 Test configuration: three views and comparison of rotors.

Experimental Setup

The rotorcraft test configuration as installed in the wind tunnel is shown in Fig. 1. The idealized airframe consists of an instrumented cylinder (134 mm diam) with a hemispherical nose. The cylinder is supported by a sting mount. Surface pressure taps along the length of the cylinder are used to measure mean surface pressures, while microphones installed in ports flush with the airframe surface are used to measure periodic (instantaneous) surface pressures relative to the mean.

The rotor is supported independently of the airframe on a drive shaft projecting downward from the tunnel ceiling. This arrangement allows the spacing to be varied between the rotor hub and the airframe. In addition, the cylinder can be moved in a streamwise direction so as to vary the relative position between the rotor plane and the airframe nose.

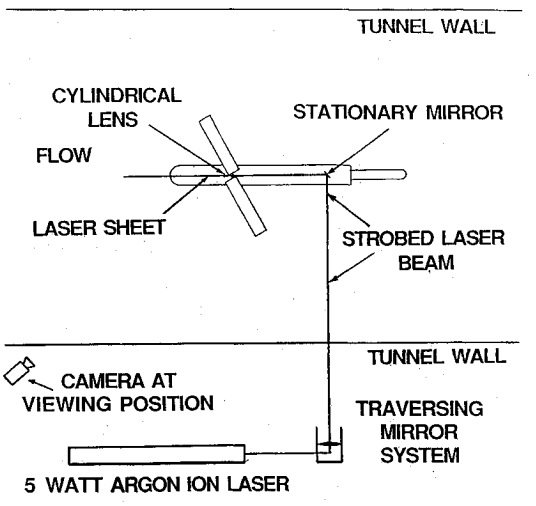

Fig. 3 Typical flow visualization setup.

Two rotors with equal radii and planform area have been used in these tests. The rotors have a solidity σ of 0.12 and a range of measured thrust coefficients from 0.00842 to 0.01096 (depending upon the advance ratio and the blade type). The blades differ in that one has a rectangular planform and the other is tapered 3:1 (Fig. 2). The tapered blade is designed to provide more uniform spanwise blade loading by creating more lift inboard than the rectangular planform does. Both rotors are very stiff, so that aerodynamic changes resulting from bending are prevented. The blades are fixed in pitch and are mounted on a simple teetering hub. The lack of controls at the hub makes for a minimum hub size, which is desirable for minimal hub interference effects. The rotor speed Ω is kept constant at 2100 rpm. The advance ratio μ is varied by changing the tunnel velocity. The simulation of forward speed is completed by a 6-deg forward tilt of the rotor shaft, as shown in Fig. 2. A complete description of the facility and the associated instrumentation is given in Ref. 11.

A typical laser sheet flow visualization arrangement is shown in Fig. 3. A 5-W argon ion laser is used to create an intense sheet of light (less than 3-mm thick) within the test section. This sheet, which is formed by a cylindrical lens positioned in the path of the laser beam, can be made to form a plane at any desired angle to the axis of the wind tunnel. The sheet is rendered visible by particles of atomized mineral oil injected into the wind-tunnel flow to reflect and scatter the laser light. The particle generator is located in the diffuser of the wind tunnel, and the particles distribute themselves uniformly throughout the closed return circuit of the wind tunnel.

The scarcity of seed particles within the tip vortex core furnishes the basis for this visualization technique. Although the flowfield is uniformly seeded, the flow associated with the rotor blade tips creates a vortex filament that contains few seed particles. When a tip vortex filament intersects the laser sheet (Fig. 4), the core of the vortex is seen as a dark spot, since few particles are within the core to scatter the light. Because the rotor wake structure is periodic, it is possible to freeze vortex core images in the light sheet by strobing the laser at the rotor frequency. In addition, images of the vortex motion can be generated as a function of rotor blade azimuth angle by shifting the strobing frequency with respect to the rotor frequency. Methods for obtaining the vortex core coor-

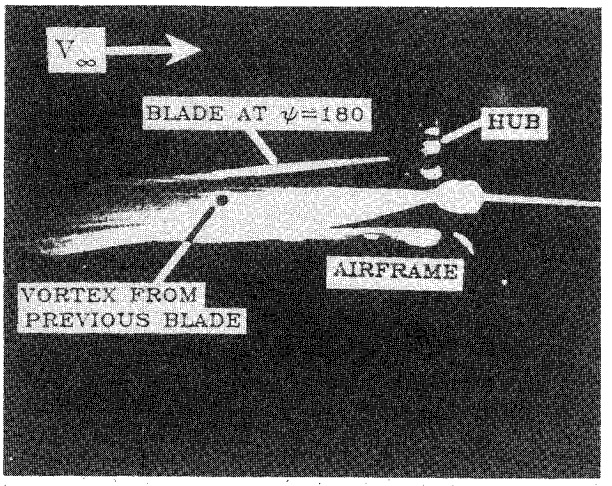

Fig. 4 Photograph of vortex core over top of airframe.

dinates in space and the corresponding rotor blade azimuth angles have been developed and are explained in Ref. 10.

Figure 3 illustrates the formation of a vertical light sheet coincident with the axis of the airframe. A photograph taken with a still camera located at the viewing position of Fig. 3 is shown in Fig. 4. The vortex core (a dark spot contrasting with the bright, uniformly seeded surroundings) was shed from the previous blade (not shown) and is moving on a trajectory above the airframe centerline.

The motion of a vortex core can be followed as the rotor blades rotate. The spatial geometry of the resulting trajectory curve can be deduced with suitable accuracy by using a precise grid superimposed on the flow visualization images. The geometric accuracy of such trajectory curves is estimated to be within 10 mm of the actual value, roughly corresponding to the vortex core radius. As the vortex core moves along the trajectory, the corresponding blade aximuth angle also may be determined. The accuracy in determining the vortex core position for a specified rotor azimuth angle is estimated to be ± 20 mm along the trajectory curve.

Laser Sheet Results and Correlations with Other Data

As can be seen from Fig. 4, the laser sheet visualization furnishes a relatively simple method for defining the flowfield in advance of laser velocimeter measurements. Thus, the boundaries of the rotor wake and the position of vortices of interest can be determined rather precisely before any point measurements are made. This greatly reduces the number of data points that must be taken with the laser velocimeter.

Velocimetry techniques, when applied to rotor flowfields, usually rely on the periodic nature of the wake structure. This is especially true for measurements near the vortex core. If a vortex core does not appear in the same spatial location for each turn of the rotor, then the measured velocity pattern becomes smeared spatially, since the data must be taken over many rotor revolutions, and the vortex is said to "jitter." With respect to flow visualization, we may define jitter as a fluctuating vortex position when the laser strobing is synchronized with the rotor frequency. Such vortex jitter was observed in this study during hover and at low advance ratio where the rotor wake hits the wind-tunnel floor. However, no jitter was observed at the advance ratios where the flow visualizations were taken. This is an important result for those engaged in taking laser velocimeter data.

The laser sheet visualization technique offers other benefits. Being able to ascertain the behavior of the rotor tip vortices from the results of the flow visualization helps to explain some of the physical features of the flow. Furthermore, correlating the flow visualization with other data sets allows for better interpretation of the data. Examples of the behavior of the rotor wake as inferred from visualization results, plus the correlation of the visualization results with other data, are presented next.

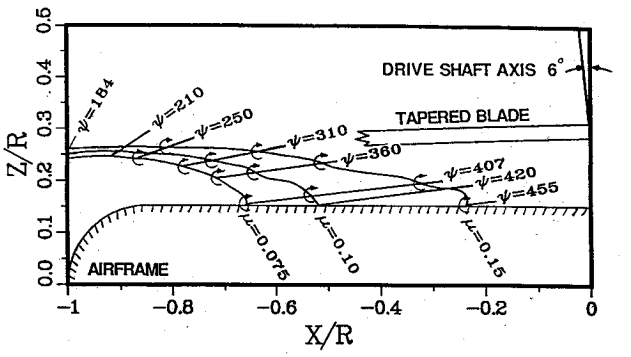

Fig. 5 Tip vortex trajectories as a function of blade azimuth angle.

Trajectories

Figure 5 shows the rotor tip vortex trajectories over the front portion of the airframe at three different advance ratios (since the rotor was run at constant rpm, these correspond to three different flight speeds). The laser sheet is positioned in the vertical plane of symmetry of the cylindrical airframe. At each flight speed, the tip vortex shed by one of the rotor blades is tracked by monitoring the behavior of the vortex cross section in the laser sheet as the vortex is swept streamwise and downward. The resulting trace in the laser sheet is a trajectory curve shown in Fig. 5. The curve begins at $X/R = -1$, which is the blade tip location when the rotor azimuth angle is 180 deg. However, the tip vortex becomes visible only when the blade trailing edge passes through the light sheet. Thus, the vortex first appears when the rotor blade is at an azimuth angle of 184 deg (since the azimuth angle is measured to the blade quarter chord by convention). Subsequent vortex positions are indicated by the corresponding blade azimuth angles as the blade proceeds to rotate about the hub. For example, at the lowest flight speed, the vortex that was shed in the vertical plane of symmetry at $Z/R = 0.24$ has moved down to $Z/R = 0.20$ when the blade associated with it has gone a further 176 deg of rotation; the vortex impinges on the airframe when the rotor blade has gone through an additional 47 deg of rotation. Similar trajectories and blade reference information appear in Fig. 5 for the other two forward flight speeds. Because the rotor is run at fixed rpm and blade pitch angle, the tip path plane adjusts slightly as the flight speed is increased (rotor flap back). Hence, there is a small vertical spacing between the three vortex trajectories at $X/R = -1.0$.

Examination of the vortex trajectory curves shows that there is a slight upflow near the front of the rotor disk. Laser velocimeter measurements[6] confirm this but also show that there is a mean upwash in this region, even in the absence of the airframe. Thus, the observed upflow behavior is attributed to effects induced by vortices that have moved downstream along the rotor wake.

When the rotor blade shedding the vortex has reached a blade azimuth angle of 360 deg, the vortex core visible in the laser sheet is said to have "aged" by 176 deg. At that time, the second rotor blade approaches the light sheet and passes over the vortex. The downwash of this second blade pushes the vortex downward rather abruptly, resulting in a bump or steepening in the vortex trajectory, as seen in Fig. 5. Also, just as the vortex is about to impinge of the surface of the airframe, the convective speed of the vortex in the X direction is sharply reduced. This results in a steep downward bend in the trajectory just before impingement. This behavior of the vortex close to the airframe can be explained on the basis of elementary vortex theory. If the surface of the cylindrical airframe is treated as being locally two-dimensional, then an image vortex system of equal and opposite strength to that of

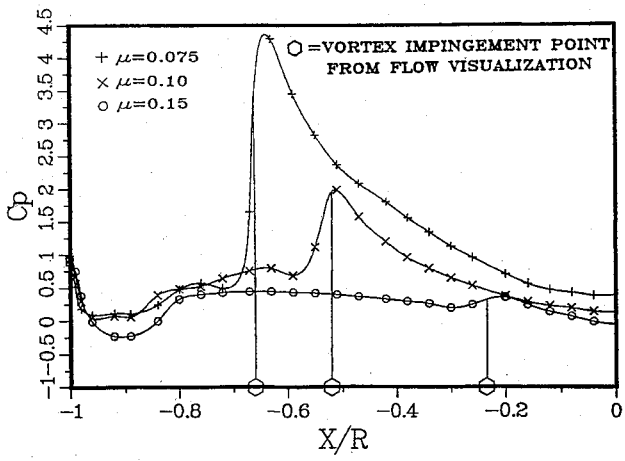

Fig. 6 Mean surface pressure variations showing the effect of rotor wake at three flight speeds.

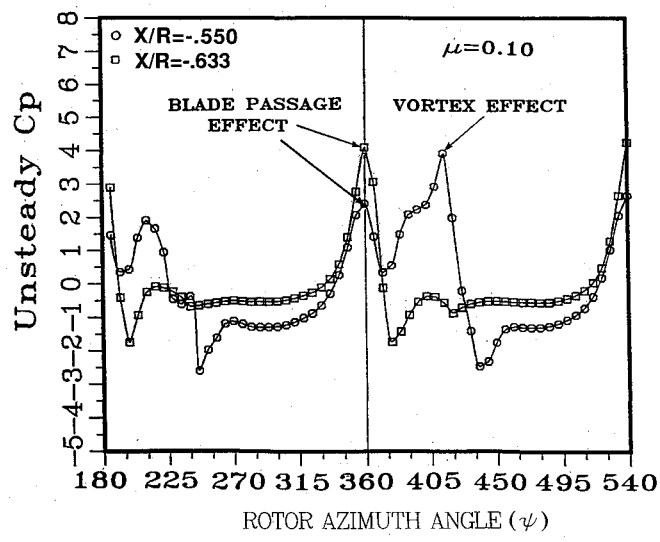

Fig. 7 Effect of vortex impingement on periodic surface pressure.

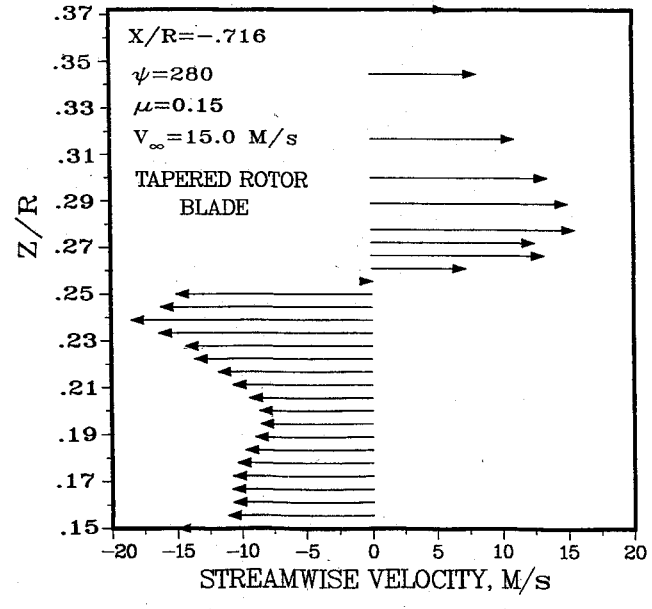

Fig. 8 Instantaneous velocities measured through tip vortex core.

the approaching vortex may be used to represent the presence of the solid surface. The sense of the image vortex is such that it would decrease the X component of velocity just above the surface and hence cause the vortex trajectory to take a steep downward bend.

Figure 5 and later figures serve to illustrate the difficulty of representing the rotor wake analytically, since the behavior of the tip vortices is so irregular in space. However, the details of the vortex geometry are both repeatable and periodic. Thus, the laser sheet visualization could be used to provide measurements for use in a prescribed wake analysis. The three trajectories in Fig. 5 represent the position of the vortex core to an estimated accuracy of ± 10 mm or to an uncertainty approximately equal to the core radius.

Correlation with Surface Pressure Data

Correlation of the flow visualization data with airframe surface pressure data is illustrated in Figs. 6 and 7. Figure 6 shows the measured mean surface pressure distribution along the top forward portion of the airframe. The pressure coefficient is normalized by the freestream dynamic pressure; hence, larger values of C_p will occur at lower flight speeds for the same value of surface pressure. Also shown in this figure is the point of vortex impingement for each of the three forward flight speeds as inferred from the laser sheet results in Fig. 5. It is seen that the sudden sharp rise in surface static pressure correlates with the point of tip vortex impingement on the surface. At the lower forward speeds, values of pressure coefficient greater than + 1 are observed both at the point of vortex impingement and downstream within the rotor wake. This indicates that energy has been added to the flow by the rotor and that much of that energy is concentrated in the tip vortices.

Figure 7 shows typical traces of the periodic pressure variation at two points on top of the airframe at a fixed value of forward speed. These traces represent fluctuations in periodic pressure about the mean value of pressure at the two stations. It is seen that the variations in pressure are substantial and that laser sheet visualization allows the the peaks in the variations to be identified with physical happenings in the flow. The pulse at $\Psi = 180$ and 360 can be correlated with blade passage over the microphones. Away from this peak, the curve for the microphone at $X/R = -0.633$ is relatively flat. However, the microphone at $X/R = -0.550$ exhibits a blade passage peak followed shortly by a peak of comparable magnitude, which can be identified from flow visualization as being due to the vortex impinging on the surface very close to this microphone.

From these typical results, it may be seen that the use of the laser sheet visualization greatly enhances the interpretation of more conventional surface pressure data.

Correlation with Velocity Data

Figure 8 represents the kinds of information that can be collected by combining the laser sheet with the laser velocimeter. First, the light sheet was used to locate a tip vortex in space at a particular freestream speed. Then a series of points was taken vertically through the vortex core with the laser velocimeter to determine the velocity profile of the core. Figure 8 shows the streamwise velocity components induced by the vortex core, relative to an observer moving with the vortex. This measurement indicates that the velocities induced by the vortex can be large, as much as 20% of the blade tip speed. Since the freestream speed is only 15% of the blade tip speed, it is not surprising that the tip vortex has such a large effect on the pressure distribution on the surface of the airframe.

The data of Fig. 8 are also useful in that they allow an experimental vortex core radius to be determined. This is valuable for analytical modeling of close vortex/surface interactions. The core radius is defined as the distance from the center of the core to the point of maximum tangential velocity. A core radius of 8 mm is deduced from the velocity measurements in Fig. 8. This value corresponds closely to the size of the particle void (i.e., the dark spot) observed in the laser sheet visualization.

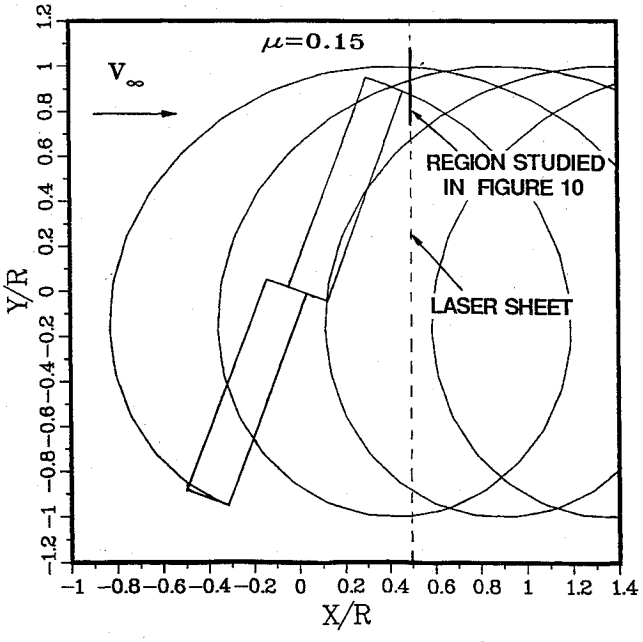

Fig. 9 Idealized rotor wake geometry for Ψ = 70.

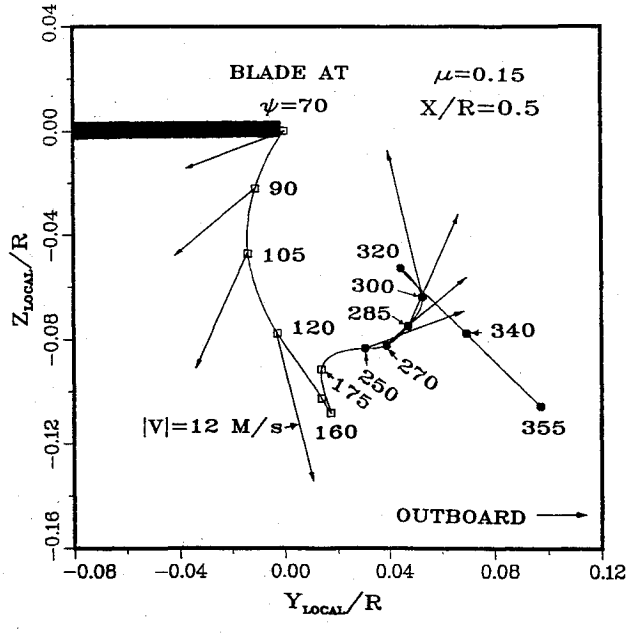

Fig. 10 Trajectory of a vortex pair near outboard edge of wake (looking upstream).

Vortex Interactions

Figure 9 presents an idealized wake geometry; that is, the tip vortex filament is assumed to move as if acted on only by the freestream, with no self-induced effects included. As one would expect, the result is a regular helix, which sweeps downstream below the rotor plane. It is noted that the filaments are closest to one another at large values of Y, i.e., at the most outboard regions of the flowfield. A measurement plane located at a large value of Y, as indicated by the dark line on Fig. 9, was studied using the rectangular planform rotor. Near this measurement plane, the vortices are close together and nearly aligned with the freestream direction. Accordingly, a laser sheet was directed across the wind tunnel test section at right angles to the axis of the airframe at $X/R = 0.50$. The cross sections of two or more vortex cores were made visible, and the motion of these cores was studied as the blade proceeded through 285 deg of rotation. The spatial behavior of two cores with respect to one another was documented, and the results are shown in Fig. 10.

The geometric origin of the coordinates in Fig. 10 is taken to be the point at which the rotor blade trailing edge exited from the laser sheet and a shed vortex first appeared. When this occurred, the rotor blade was near an azimuth angle of 70 deg. The position of the shed vortex at this instant is shown by a square, open symbol at the origin of the coordinates. Also shown in the figure, and denoted by a circular, closed symbol labeled $\Psi = 250$, is the location (at the same instant) of the vortex core generated 180 deg earlier by the previous rotor blade. The subsequent trajectories traced by the pair of vortices are shown in Fig. 10, with the simultaneous vortex core positions denoted by paired solid and open symbols separated by 180 deg.

The simple wake model of Fig. 9 indicates that the blade tip vortex should initially move outboard as the rotor blade continues past the laser sheet. The behavior of the vortex from $\Psi = 70$ to 105 is just the opposite. It is apparent that the induced effects of the vortices on one another can be substantial. In an attempt to quantify this effect, the induced vortex velocity field was evaluated from Fig. 8 and applied at the vortex core locations denoted with paired solid and open symbols in Fig. 10. (Although the tip vortex strength varies between the tapered and rectangular blade and also with rotor blade azimuth angle, the vortex velocity distribution measured from Fig. 8 was taken as being representative of the strength of the vortices discussed here.) In Fig. 10, a velocity vector shown induced at a core location with an open symbol is due to the companion vortex with the closed symbol, and vice versa. It is apparent that this approach is not sufficient to explain the observed behavior of the tip vortex. The behavior may be explained on the basis of "secondary vortex generation," observed by Larin.[12] This phenomenon is associated with strong interactions between neighboring vortex filaments. The individual filaments become severly distorted, looping over one another and creating an extremely complex three-dimensional vortex system at the outboard edges of the rotor wake. It should be emphasized that the trajectories shown in Fig. 10 are repeatable in a periodic sense. As one tip vortex moves to its location at $\Psi = 250$, another appears at the tip, and when the first vortex moves onward to $\Psi = 430$, yet another appears at the tip. This pattern is repeated every rotor half-revolution, and the location of the vortices in space for any given value of Ψ is remarkably consistent. These results demonstrate the extreme complexity of the rotor wake.

Airframe Effects

The ability of the laser sheet to document a rotor wake is shown in Fig. 11. This figure is a composite of information obtained from vertical laser light sheets aligned parallel with the airframe axis and moved to 10 different Y/R stations. Vortex core coordinates having common rotor blade azimuth angles were connected at the various Y/R stations, revealing the instantaneous vortex filament shapes and locations as shown. Actually, because a two-bladed rotor was used, only vortex filaments 180 deg apart in age exist simultaneously. For instance, the tip vortex filament present at 210 deg coexists with the filament labeled 390 deg, which was shed from the previous blade. Figure 11 represents a top view of the rotor wake over the forward portion of the airframe. The dashed lines represent the location of the vortex wake as predicted by the simple method discussed with reference to Fig. 9, whereas the solid lines represent filaments derived from visualization. The measured vortex filaments are seen to convect downstream faster than the idealized vortex filaments. This is due to wake contraction occurring within the nonideal wake.

Relative to the idealized wake, the progression of filaments in Fig. 11 shows increasing distortion as the solid boundary of the airframe is approached. Portions of the filaments that are above the airframe appear to move more slowly in the streamwise direction than do those portions of the filaments outboard of the airframe. Such a behavior was noted earlier, in

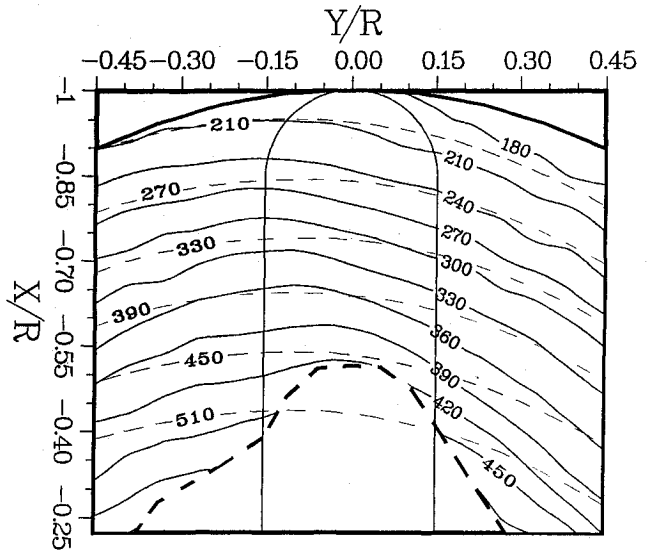

Fig. 11 Comparison of idealized tip vortex geometry with visualized geometry ($\mu = 0.10$).

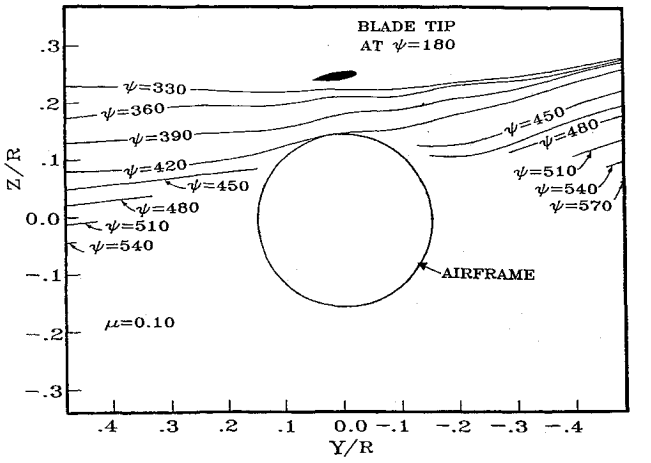

Fig. 12 Front view of tip vortex filaments obtained from flow visualization.

the discussion of vortex trajectories above the airframe, and is attributed to the vorticity distribution set up on the airframe surface by the approaching vortex filament.

Inside the region to the right of the heavy dashed line in Fig. 11, no vortex core was observed. It appears that the filament is cut and that each end passes independently down the side of the airframe. Figure 12, a cross plot of the data in Fig. 11, shows what happens to the vortex filaments with respect to a vertical plane. The vortex filaments appear to terminate in space as observed in the flow visualization. That is, the vortex core loses its definition and can no longer be tracked. It appears that the vortex impingement on the airframe precipitates vortex breakdown. The core rapidly entrains seed particles as it diffuses, rendering it invisible to the laser sheet. A comprehensive description of the wake geometry, such as is presented in Figs. 11 and 12, should be useful to those attempting to model the rotor-airframe aerodynamics.

Concluding Remarks

As a result of the flow visualization experiments carried out with the laser sheet technique, the following conclusions may be drawn:

1) The laser sheet technique is a powerful and relatively simple method for visualizing the details of the periodic rotor wake.

2) Quantitative results may be derived from the visualization with satisfactory accuracy.

3) Laser sheet flow visualization allows for correlations with other data to be made. Thus, this visualization technique is extremely useful for interpreting point measurements.

4) Details of the tip vortex geometry are periodic and repeatable.

5) The behavior of the rotor tip vortex is strongly affected by the presence of the airframe.

6) The motion of the tip vortex is strongly affected by the presence of other nearby vortices from other blades or from previous revolutions.

7) Vortex interaction with the surface of the airframe results in a sudden loss of vortex core definition. The tip vortex is not observable as a distinct flow feature below the airframe.

Acknowledgments

The research was sponsored by the U.S. Army Center of Excellence for Rotary Wing Aircraft Technology under Contract No. DAAG-29-82-K-0084. The contract monitors were Dr. Robert Singleton and Dr. Thomas Doligalski. The authors gratefully acknowledge the assistance of Mr. S. G. Liou, who was responsible for the laser velocimeter measurements.

References

[1]Sheridan, P. F. and Smith, R. P., "Interactional Aerodynamics—A New Challenge to the Helicopter Industry," *AHS Journal,* Vol. 25, Jan. 1980, pp. 3–21.

[2]Phillipe, J. J., Roesch, P., Dequin, A., and Cler, A., "A Survey of Recent Developments in Helicopter Aerodynamics," AGARD Lecture Series No. 139, *Helicopter Aeromechanics,* May 1985.

[3]Egolf, T. A. and Lorber, P. F., "An Unsteady Rotor/Fuselage Interaction Method," *Proceedings of the American Helicopter Society Specialists' Meeting,* Arlington, TX, Feb. 1987.

[4]Brand, A. G., McMahon, H. M., and Komerath, N. M., "Surface Pressure Measurements on a Body Subject to Vortex Wake Interaction," *AIAA Journal* (to be published).

[5]McMahon, H. M., Komerath, N. K., and Hubbartt, J. E., "Studies of Rotor-Airframe Interactions in Forward Flight," AIAA Paper 85-5015, Oct. 1985.

[6]Liou, S. G., Komerath, N. M., and McMahon, H. M., "The Velocity Field of a Lifting Rotor in Low-Speed Forward Flight," AIAA Paper 88-0666, Jan. 1988.

[7]Veret, C., "Flow Visualization by Light Sheet," *Flow Visualization III,* edited by W. J. Yang, Hemisphere, Washington, DC, 1985.

[8]Porcar, R., Prenel, J., Diemunsch, G., and Hamelin, P., "Visualizations by Means of Coherent Light Sheets; Applications For Various Flows," *Flow Visualization III,* edited by W. J. Yang, Hemisphere, Washington, DC, 1985, pp. 123–127.

[9]McGregor, I., "The Vapor-Screen Method of Flow Visualization," *Journal of Fluid Mechanics,* Vol. 11, 1969, pp. 481–511.

[10]Brand, A. G., Komerath, N. M., and McMahon, H. M., "A Laser Sheet Technique for Visualizing a Periodic Rotor Wake," *Journal of Aircraft,* Vol. 25, July 1988, pp. 667–668.

[11]Brand, A. G., McMahon, H. M., and Komerath, N. M., "Wind Tunnel Data from a Rotorcraft/Airframe Interaction Study," School of Aerospace Engineering, Georgia Institute of Technology, Atlanta, Contract DAAG29-82-K-0094, July 1986.

[12]Larin, A., "Vortex Wake Behind a Helicopter," *Aviatsiyai Kosmoncutike,* No. 3, 1973, pp. 32–33.